

# Temperature compensation method of silicon microgyroscope based on BP neural network

Xia Dunzhu Wang Shourong Zhou Bailing

(Key Laboratory of Micro-Inertial Instrument and Advanced Navigation Technology of Ministry of Education, Southeast University, Nanjing 210096, China)

**Abstract:** The temperature characteristics of a silicon microgyroscope are studied, and the temperature compensation method of the silicon microgyroscope is proposed. First, an open-loop circuit is adopted to test the entire microgyroscope's resonant frequency and quality factor variations over temperature, and the zero bias changing trend over temperature is measured via a closed-loop circuit. Then, in order to alleviate the temperature effects on the performance of the microgyroscope, a kind of temperature compensated method based on the error back propagation (BP) neural network is proposed. By the Matlab simulation, the optimal temperature compensation model based on the BP neural network is well trained after four steps, and the objective error of the microgyroscope's zero bias can achieve 0.001 in full temperature range. By the experiment, the real time operation results of the compensation method demonstrate that the maximum zero bias of the microgyroscope can be decreased from 12.43 to 0.75 ( $^{\circ}$ )/s after compensation when the ambient temperature varies from  $-40$  to  $80$   $^{\circ}\text{C}$ , which greatly improves the zero bias stability performance of the microgyroscope.

**Key words:** silicon microgyroscope; temperature characteristic; error back propagation neural network; temperature compensation

Over the past decades, the silicon microgyroscope has become an emerging kind of inertial sensor, which is widely applied in the fields of navigation, control and positioning<sup>[1-3]</sup>. Due to the characteristics such as small size, light weight, high reliability and low costs, it is convenient to achieve digitalization and intellectualization, and it is suitable for mass production. However, the resonant frequencies and quality factors in drive and sense modes are prone to be affected by the ambient temperature, which can lead to the zero bias fluctuation and further reduce its zero bias instability.

The temperature error mechanisms of the microgyroscopes with tuning type and angular vibrating type are investigated from the aspect of the systematic Brownian noise; however, the Brownian noise only determines the resolution of the microgyroscope and has little impact on the zero bias error<sup>[4-5]</sup>. The systematic identification is accomplished by some testing methods, and the temperature error mechanism of the microgyroscope is mainly analyzed in terms of the structural resonant frequency variation induced by temperature chan-

ges<sup>[6]</sup>. The temperature model of the silicon microgyroscope is deduced according to Seebeck effects of silicon material, but it only discusses the temperature error caused by Young's modulus changes over the temperature variations<sup>[7]</sup>. The temperature dependent drifts and the noise characteristics of packaged silicon microgyroscopes are well investigated. The resonant frequency, quality factor, AGC voltage and signal drifts are all subjected to various temperature environments from  $-60$  to  $60$   $^{\circ}\text{C}$ <sup>[8]</sup>. However, there are no effective schemes suggested for systematic temperature compensations.

Theoretically, the spring coefficient of the microgyroscope supporting beam changes with the temperature variation owing to Young's modulus changing over temperature. According to the kinetic equation, the resonant frequency of the microgyroscope is relevant to the sensitivity, stability and dynamic characteristics; thus, the temperature variation has significant effects on both the output sensitivity and the stability as well as the dynamic characteristics of the microgyroscope, resulting in the complex temperature drifts of the entire system. Therefore, the temperature compensation method is proposed to improve the overall performance of the microgyroscope.

## 1 Temperature Characteristics of Microgyroscope

Fig. 1 shows the temperature characteristics test setup of the microgyroscope, including the open-loop and the closed-loop circuits. The waveform generator provides the sinusoidal signal to drive the microgyroscope, and the signal output is recorded by connecting to multimeters, oscilloscope and spectrum analyzer, respectively. The temperature control chamber is used to provide the testing ambient temperature.

First of all, an open-loop driving circuit is adopted to test the microgyroscope's resonant frequency and the quality factor under the circumstance of temperature varying from  $-40$  to  $60$   $^{\circ}\text{C}$ . During the measurement, the microgyroscope and

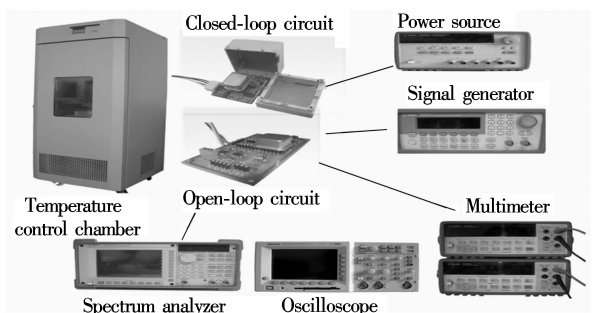


Fig. 1 Temperature characteristics test setup of microgyroscope

Received 2009-06-25.

**Biography:** Xia Dunzhu (1978—), male, doctor, xiadz\_1999@163.com.

**Foundation items:** The National High Technology Research and Development Program of China (863 Program) (No. 2002AA812038), the National Natural Science Foundation of China (No. 60974116).

**Citation:** Xia Dunzhu, Wang Shourong, Zhou Bailing. Temperature compensation method of silicon microgyroscope based on BP neural network[J]. Journal of Southeast University (English Edition), 2010, 26(1): 58 – 61.

the circuit are statically mounted, and the set temperature in the temperature control chamber varies from  $-40$  to  $60$  °C by intervals of  $10$  °C. The temperature at each sampling point is maintained for 60 min before testing to ensure that the temperature in the chamber is uniformly distributed and the microgyroscope is fully heated. Therefore, the lag between the inner temperature and the outer temperature of the microgyroscope can be effectively avoided. The testing results are shown in Fig. 2 to Fig. 5.

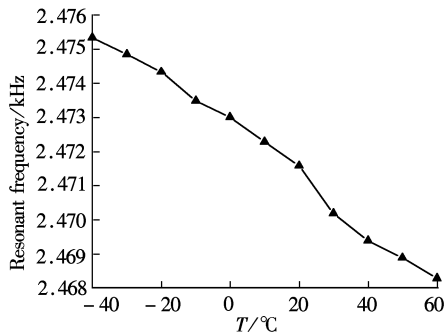


Fig. 2 Trend of resonant frequency vs.  $T$  in drive mode

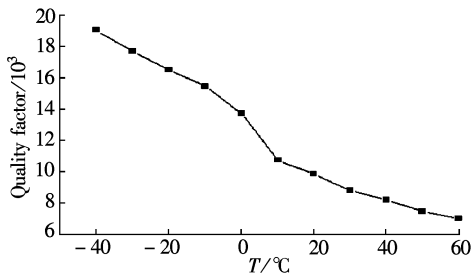


Fig. 3 Trend of quality factor vs.  $T$  in drive mode

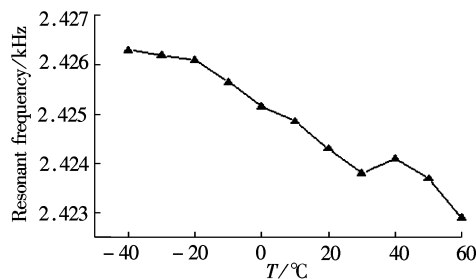


Fig. 4 Trend of resonant frequency vs.  $T$  in sense mode

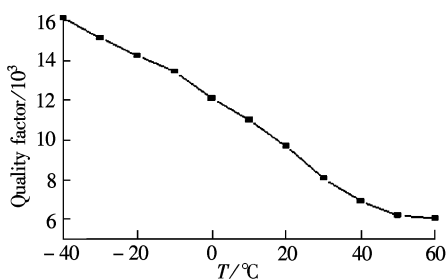


Fig. 5 Trend of quality factor vs.  $T$  in sense mode

According to the data in Fig. 2 and Fig. 4, the resonant frequencies in drive and sense modes both decrease nearly linearly when the temperature increases, and their variable magnitudes are within 10 Hz from  $-40$  to  $60$  °C. It is noticeable from Fig. 3 and Fig. 5 that the quality factor drastically drops in the range of low temperature, which is much higher than that of normal temperature. Moreover, its chan-

ging tendency mitigates when the temperature rises higher than  $30$  °C. The reason is that most of the little residual gas inside the vacuum-packaged microgyroscope is absorbed under the low temperature, and it is released when the temperature ascends. However, only a little limited gas is absorbed in the vacuum packaged microgyroscope; therefore, the quality factor varies slowly since only a little gas is released when the temperature increases.

Actually, the microgyroscope is tested by using manual operation via an open-loop circuit to record its intrinsic structural features. However, to achieve the overall prototype realization and track the driving resonant frequency automatically in accordance with the open-loop situation, a closed-loop circuit is designed to accomplish the function. Moreover, the zero bias is closely related to the resonant frequencies and quality factors in drive and sense modes<sup>[7-8]</sup>. Though the resonant frequencies and quality factors cannot be compensated for, the key sensor performance, i. e., the zero bias output, is effectively compensated for.

The second step is to test the performances of the integrated microgyroscope by the closed-loop driving circuit. First, the microgyroscope is still placed in the temperature control chamber, and its closed-loop driving amplitude and zero bias are measured when the temperature varies from  $-40$  to  $60$  °C with one step of  $20$  °C. Then the temperature is kept for one hour at each testing point, which can ensure that the microgyroscope is fully heated and the temperature field inside the microgyroscope is homogeneously distributed. At each temperature point it takes one hour to reach a thermal balance before the recording of the zero bias of the microgyroscope, each temperature point is recorded for about 3 h in Fig. 6. Then the average output of the microgyroscope at each temperature point is calculated and fitted by the polygonal line in Fig. 7. Thus the overall trend zero bias over temperature changes can be clearly exhibited. Data 1, Data 2 and Data 3 are three different groups of tests well indica-

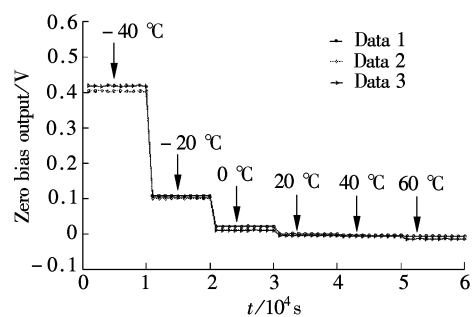


Fig. 6 Closed-loop test of zero bias of microscope over temperature changes

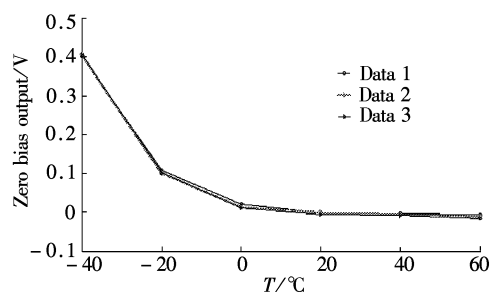


Fig. 7 Trend of zero bias change over temperature

ting an excellent repeatability.

## 2 Temperature Compensation Method Based on BP Neural Network

From the above testing experiments, we can acquire some important temperature characteristics of the microgyroscope designed in our laboratory, which can provide the useful proof for compensation.

The adopted BP neural network structure is shown in Fig. 8.  $T$  is the input temperature value for training and processing;  $w_i (i = 1, 2, \dots, 10)$  is the weight value connecting the input layer and the hidden layer;  $b_i (i = 1, 2, \dots, 10)$  is

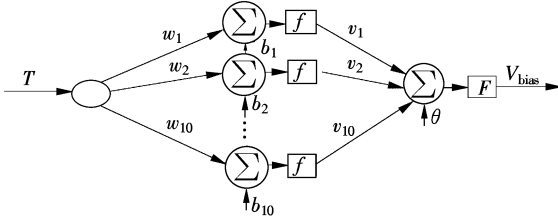


Fig. 8 Structure of BP neural network adopted for modeling

the corresponding threshold value;  $f$  is the tan-sigmoid transfer function;  $v_j (j = 1, 2, \dots, 10)$  is the weight value connecting the hidden layer and the output layer;  $\theta$  is the corresponding threshold value;  $F$  is the linear-sigmoid transfer function; and  $V_{\text{bias}}$  is the final output for the zero bias compensation. Moreover, in order to speed up convergence and reduce the error, the TRAINLM function is adopted in the training. In the training, the temperature  $T$  is the input value and the corresponding zero bias of the microgyroscope  $V_{\text{bias}}$  is the output value. Through the reversal Levenberg-Marquadt algorithm, we set the maximum twelve training steps and the training target error approaches 0.001.

In this case, both the input layer and the output layer have only one neural cell, while the hidden layer has 10 neural cells so as to attain a higher fitting precision and a forecast precision. Tab. 1 summarizes the adopted Matlab neural network tools, i. e., the recalled functions during the programming. Tab. 2 records the relationship between the zero bias and the temperature when the scale factor of the tested microgyroscope is  $8.774 \text{ mV}/((^\circ) \cdot \text{s}^{-1})$ .

Tab. 1 Neural network Matlab functions

Matlab function	Description
$[T_n, \min T, \max T, b_n, \min b, \max b] = \text{premnmx}(T, \text{bias})$	Normalize the input and output value
$\text{net} = \text{newff}(\text{minmax}(T_n), [s, 1], \{\text{'tansig'}, \text{'purelin'}\}, \text{'trainlm'})$	Construct BP neural network
$\text{net.trainParam.epochs} = 100$	Set the maximum training steps
$\text{net.trainParam.goal} = 0.001$	Set the objective error
$\text{net} = \text{train}(\text{net}, T_n, b_n)$	Start training

Tab. 2 Uncompensated zero bias of microgyroscope over temperature

Temperature/ $^\circ\text{C}$	Average voltage output/mV	Zero bias/ $((^\circ) \cdot \text{s}^{-1})$	Temperature/ $^\circ\text{C}$	Average voltage output/mV	Zero bias/ $((^\circ) \cdot \text{s}^{-1})$
80	52.7	6.01	15	88.3	10.06
75	52.2	5.95	10	94.2	10.74
70	53.2	6.06	5	98.4	11.21
65	53.5	6.10	0	102.7	11.71
60	52.4	5.97	-5	103.5	11.80
55	50.3	5.73	-10	105.7	12.05
50	51.6	5.88	-15	108.9	12.41
45	54.5	6.21	-20	109.1	12.43
40	60.6	6.91	-25	108.2	12.33
35	68.4	7.79	-30	107.5	12.25
30	74.4	8.48	-35	105.9	12.07
25	79.9	9.11	-40	98.1	11.18
20	85.8	9.77			

As shown in Fig. 9(a), the training target error results can meet the requirement after only four times training. Finally, all the trained networks' weights and threshold values are preserved as constant coefficients, and thus the BP neural network of the temperature model is successfully built. The final training simulation result of the model is shown in Fig. 9(b).

After the network model is built up, the current temperature is used as the input value to obtain the corresponding zero bias for compensation. Then it is subtracted by the actual output to obtain the compensated zero bias of the microgyroscope. In the Matlab simulation, the original temperature is substituted to obtain the compensated zero bias curve,

which is obviously near zero and almost becomes a straight line in Fig. 9(b).

In order to verify the effectiveness of the compensating model, the microgyroscope is put in the thermal control chamber. The ambient temperature is controlled to increase from  $-40$  to  $80$   $^\circ\text{C}$  at the step of  $10$   $^\circ\text{C}$ . At each temperature point the zero bias is recorded for 30 min; thus, the compensated zero bias curve is obtained through the on-line compensating model in the computer. As shown in Fig. 10, the maximum zero bias decreases remarkably from  $12.43$   $(^\circ)/\text{s}$  (before compensation) to  $0.75$   $(^\circ)/\text{s}$  (after compensation), which can provide comparable references for other compensating methods.

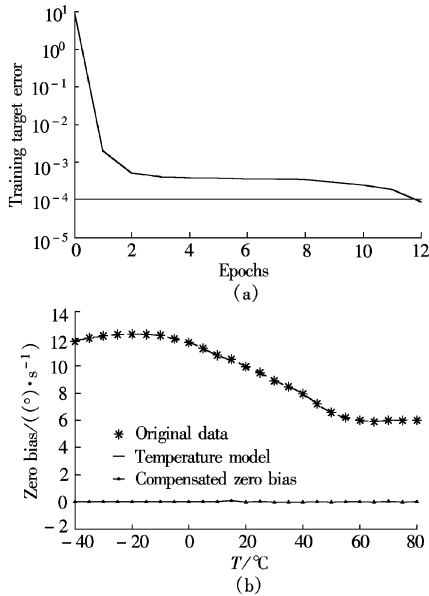


Fig. 9 Training of network and simulation result. (a) BP neural network training; (b) Zero bias vs. temperature

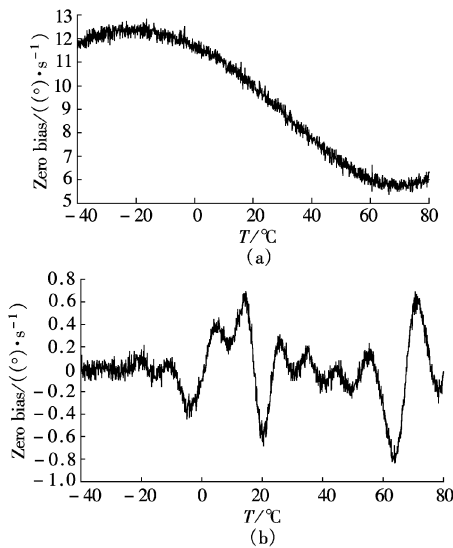


Fig. 10 Verification of BP neural network's compensation effects. (a) Before compensation; (b) After compensation

### 3 Conclusion

The performance of the microgyroscope is greatly affected by temperature variations. In this paper, the temperature testing results reveal the temperature characteristics of the microgyroscope. The resonant frequency and quality factor variations over the temperature can indirectly influence the zero bias output and its stability. To reduce the microgyroscope's zero bias drifts over temperature, the temperature compensation method is proposed and carried out, and the experimental results are given.

### References

- [1] Sharma A, Zaman M F, Ayazi F. A 0.2 $^\circ$ /hr micro-gyroscope with automatic CMOS mode matching [C]//*Proc of the IEEE International Solid-State Circuits Conference*. San Francisco, CA, USA, 2007: 386-387.
- [2] Kulygin A, Schmid U, Seidel H. Characterization of a novel micromachined gyroscope under varying ambient pressure conditions [J]. *Sens Actuators A: Phys*, 2008, **145**(1): 52-58.
- [3] Li Z, Yang Z, Xiao Z. A bulk micromachined vibratory lateral gyroscope fabricated with wafer bonding and deep trench etching [J]. *Sens Actuators A: Phys*, 2000, **83**(1): 24-29.
- [4] Ashwin A S. Integrated micromechanical resonant sensor for inertial measurement system [D]. Berkeley, CA, USA: School of Electrical Engineering and Computer Science of University of California at Berkeley, 2002.
- [5] Wyatt O D. Mechanical analysis and design of vibratory micromachined gyroscopes [D]. Berkeley, CA, USA: School of Mechanical Engineering of University of California at Berkeley, 2001.
- [6] Jason K P H. Modeling and identification of the jet propulsion laboratory vibratory rate microgyroscope [D]. Los Angeles: School of Mechanical Engineering of University of California at Los Angeles, 2002.
- [7] Fang Jiancheng, Li Jianli, Sheng Wei. Improved temperature error model of silicon MEMS gyroscope with inside frame driving [J]. *J Beijing Univ Aeronaut Astronaut*, 2006, **32**(11): 1277-1280. (in Chinese)
- [8] Shcheglov K, Evans C, Gutierrez R, et al. Temperature dependent characteristics of the JPL silicon MEMS gyroscope [C]//*Proceedings of the IEEE Aerospace Conference*. Big Sky, MT, USA, 2000: 403-411.

## 基于 BP 神经网络的硅微陀螺仪温度补偿方法

夏敦柱 王寿荣 周百令

(东南大学微惯性仪表与先进导航技术教育部重点实验室, 南京 210096)

**摘要:** 研究了硅微陀螺的温度特性, 提出了硅微陀螺仪的温度补偿方法. 首先, 采用开环电路测试了微陀螺仪的谐振频率和品质因素随温度变化的情况, 并采用闭环电路测试了微陀螺整机零偏随温度变化规律. 然后, 为研究降低温度对微陀螺性能的影响, 提出了一种基于误差反向传播 (BP) 神经网络的温度补偿方法. 通过 Matlab 仿真, 基于 BP 神经网络温度补偿的优化模型经过 4 步就得到很好训练, 并使全温范围内微陀螺零偏的目标误差达到 0.001. 该补偿方法实时运行试验结果表明, 环境温度在 -40 ~ 80  $^\circ C$  变化过程中, 微陀螺仪的最大零偏经过补偿能从 12.43  $(^\circ)/s$  降低到 0.75  $(^\circ)/s$ , 从而大大提高了微陀螺仪的零偏稳定性.

**关键词:** 硅微陀螺仪; 温度特性; 误差反向传播神经网络; 温度补偿

**中图分类号:** U666.112